KRIT1, a gene mutated in cerebral cavernous malformation, encodes a microtubule-associated protein

Murat Gunel*, Maxwell S. H. Laurans*†, Dana Shin*†, Michael L. DiLuna*†, Jennifer Voorhees*, Keith Choate†, Carol Nelson-Williams†, and Richard P. Lifton†‡

*Department of Neurosurgery, Yale Neurovascular Surgery Program, and †Department of Genetics, Howard Hughes Medical Institute, Yale University School of Medicine, 333 Cedar Street, New Haven, CT 06510

Contributed by Richard P. Lifton, June 12, 2002

Mutations in Krev1 interaction trapped gene 1 (*KRIT1*) cause cerebral cavernous malformation, an autosomal dominant disease featuring malformation of cerebral capillaries resulting in cerebral hemorrhage, strokes, and seizures. The biological functions of *KRIT1* are unknown. We have investigated KRIT1 expression in endothelial cells by using specific anti-KRIT1 antibodies. By both microscopy and coimmunoprecipitation, we show that KRIT1 co-localizes with microtubules. In interphase cells, KRIT1 is found along the length of microtubules. During metaphase, KRIT1 is located on spindle pole bodies and the mitotic spindle. During late phases of mitosis, KRIT1 localizes in a pattern indicative of association with microtubule plus ends. In anaphase, the plus ends of the interpolar microtubules show strong KRIT1 staining and, in late telophase, KRIT1 stains the midbody remnant most strongly; this is the site of cytokinesis where plus ends of microtubules from dividing cells overlap. These results establish that KRIT1 is a microtubule-associated protein; its location at plus ends in mitosis suggests a possible role in microtubule targeting. These findings, coupled with evidence of interaction of KRIT1 with Krev1 and integrin cytoplasmic domain-associated protein-1 alpha (ICAP1 α), suggest that KRIT1 may help determine endothelial cell shape and function in response to cell–cell and cell–matrix interactions by guiding cytoskeletal structure. We propose that the loss of this targeting function leads to abnormal endothelial tube formation, thereby explaining the mechanism of formation of cerebral cavernous malformation (CCM) lesions.

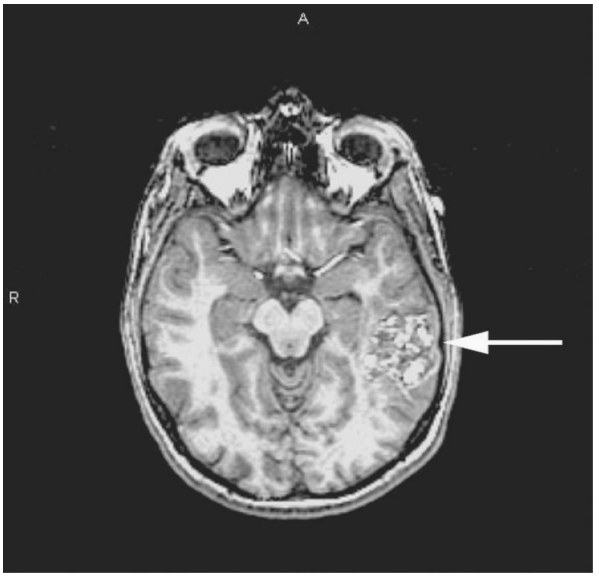

Fig. 1. MRI appearance of CCM. Axial MRI view of the brain. Characteristic cavernous malformation lesion (marked with arrow) is seen within the left temporal lobe. The heterogeneous signal within the lesion is indicative of prior hemorrhage.

Cerebral cavernous malformation (CCM) is a disease affecting brain vasculature. Characteristic lesions affect capillaries and have grossly dilated vascular channels lined by only a single layer of endothelium without normal vessel wall elements such as smooth muscle or intervening neural parenchyma (1). The nature of these lesions suggests an abnormality in normal development of these capillaries; however, the mechanism of their occurrence and an explanation for their focal nature have remained elusive.

The aberrant channels in CCM lesions are fragile, commonly resulting in intracranial hemorrhage. Clinical signs and symptoms are largely determined by the size and location of the hemorrhage, and range from incidental findings on MRI (Fig. 1) to rare catastrophic cerebral hemorrhage resulting in death. The disease has been recognized as a common clinical entity because of the advent of MRI (2). Both MRI and autopsy studies suggest a prevalence of cavernous malformation up to 0.5%, although only 20–30% of affected individuals develop symptomatic disease (3–8). Symptomatic patients typically present in the third through the fifth decades of life (3) with headaches, seizures, or focal neurological deficits. Treatment ranges from therapy with anti-epileptic drugs in patients with seizures, to surgical excision of accessible lesions in patients who suffer from hemorrhage or intractable seizures (9–13).

Since its initial description, CCM has been recognized to be a heritable disorder (14–16). Genetic analysis of kindreds with familial CCM has mapped three autosomal dominant loci causing this disease. *CCM1* is located at 7q21 (17–21), *CCM2* at 7p13–15 (18), and *CCM3* at 3q25–27 (18). Apparent loss of function mutations in *KRIT1* (Krev1 interaction trapped gene 1) have recently been shown to be the cause of disease mapping to *CCM1* (22–27); the genes underlying *CCM2* and *CCM3* have not yet been identified.

The normal function of KRIT1 and the mechanism by which its mutation causes CCM is not known. This gene was initially identified and cloned in a yeast two-hybrid screen by using *Krev1 (Rap1A)*, which encodes a small GTPase with significant sequence homology to *Ras* (28). Although the Ras pathway has been implicated in angiogenesis (29), the relationship between Ras, Krev1, and KRIT1 has not been established. Recent publications have identified another interacting partner, integrin cytoplasmic domain-associated protein-1 α (ICAP1 α) (30, 31).

The histology of cavernous malformations suggests that KRIT1 may play a central role in normal vascular development

Abbreviations: CCM, cerebral cavernous malformation; *KRIT1*, Krev1 interaction trapped gene 1; BAEC, bovine aortic endothelial cell; RT, reverse transcription; ICAP1 α, integrin cytoplasmic-associated protein-1 α.

‡To whom reprint requests should be addressed at: Yale University School of Medicine, Howard Hughes Medical Institute, 295 Congress Avenue, BCMM 154D, New Haven, CT 06510. E-mail: Richard.Lifton@yale.edu.

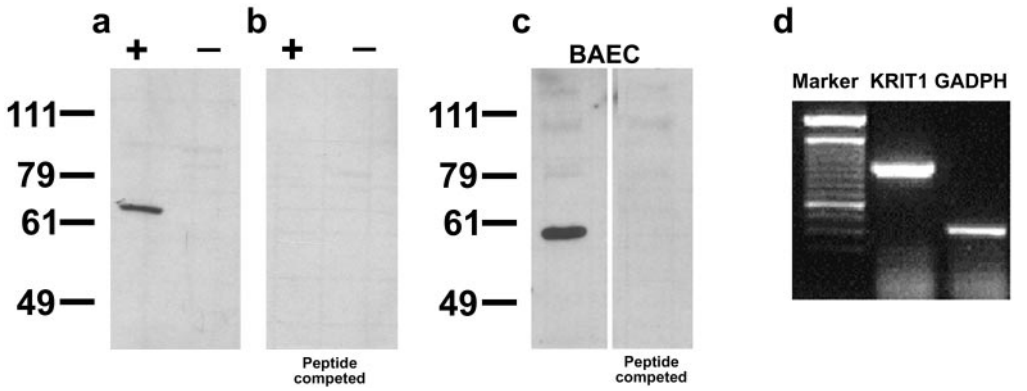

Fig. 2. KRIT1 mRNA and protein are expressed by BAEC cultures. Anti-KRIT1 antibodies were used to stain Western blots of extracts of COS7 cells (*a* and *b*). These cells, which do not express endogenous KRIT1, were transfected either with plasmid expressing His-tagged KRIT1 (+) or an empty vector (−) as described in *Methods*. (*a*) Staining detected a protein of size expected for the fusion protein in cells transfected with KRIT1. (*b*) Peptide competition eliminates staining, demonstrating the specificity of this antibody for the KRIT1 protein. (*c*) Western blot of native BAECs using anti-KRIT1. A 58-kDa band is detected when protein isolated from BAEC cultures is probed with anti-KRIT1 antibodies; this band is competed by the immunizing peptide. (*d*) RT-PCR reveals *KRIT1* mRNA expression in BAECs. The sequence of the product reveals an encoded protein of 85% identity with human KRIT1.

or in maintenance of vascular integrity. To address this question, we have studied the expression and localization of KRIT1 in bovine aortic endothelial cells (BAECs).

Methods

***In Vitro* Cultures.** BAECs [American Type Culture Collection (ATCC), Manassas, VA] at early passages (<6) were cultured in high glucose DMEM (GIBCO/BRL) with 10% FBS, 100 mM Hepes, 10 mM sodium pyruvate, 100 units·ml^{-1} penicillin G, 100 mg·ml^{-1} streptomycin, and 0.25 mg·ml^{-1} amphotericin B. COS7 cells were grown in low glucose DMEM with 10% FBS and 100 units·ml^{-1} penicillin G, 100 mg·ml^{-1} streptomycin, and 0.25 mg·ml^{-1} amphotericin B. Cells harvested for Western blot and reverse transcription (RT)-PCR analysis were seeded on

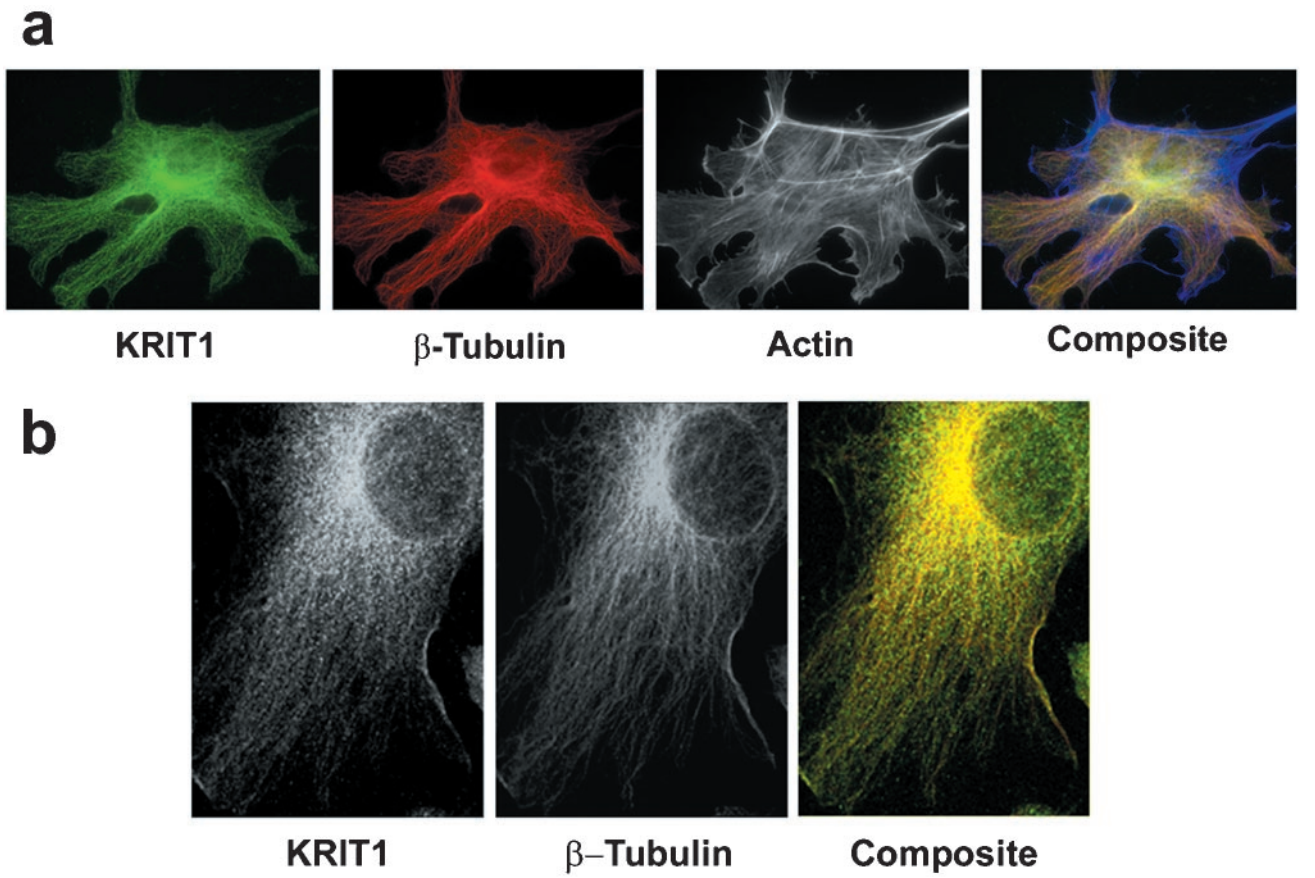

Fig. 3. Immunocytochemistry of endothelial cells. BAECs were stained with antibodies to KRIT1, actin, and β-tubulin. (*a*) KRIT1 staining reveals a filamentous pattern that differs from actin staining but overlaps with that of β-tubulin; magnification ×63. (*b*) Confocal image demonstrates colocalization of KRIT1 with β-tubulin; magnification ×63. KRIT1 staining was competed by the immunizing peptide (data not shown).

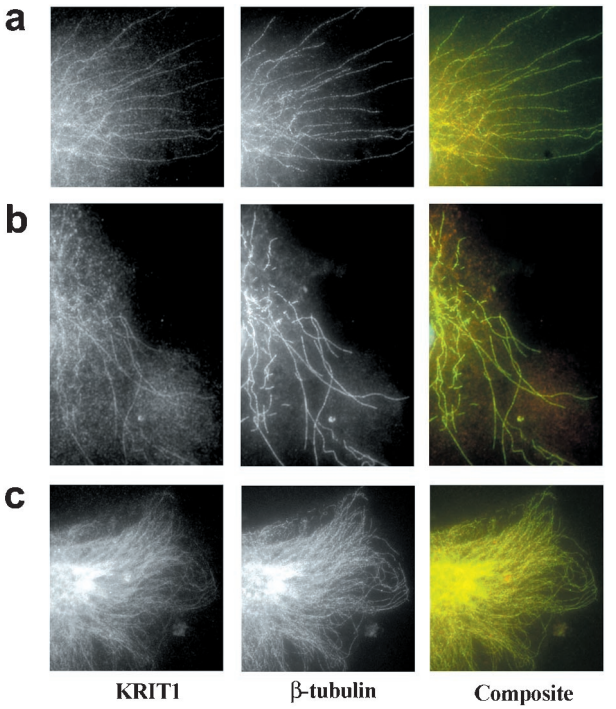

Fig. 4. Colocalization of KRIT1 and β-tubulin after cold treatment. After indicated treatments of cultured BAECs, cells were stained for KRIT1 and β-tubulin. After 5 min (*a*) or 20 min (*b*) on ice, disruption of microtubules is observed, affecting both β-tubulin and KRIT1 staining. After 20 min of recovery at 37°C, microtubules have repolymerized, and KRIT1 staining is seen along their length (*c*).

100-mm dishes at a concentration of 1×10^7 cells per dish and grown to confluence.

RT-PCR. Total cellular RNA was extracted from cells grown in tissue culture dishes by using Trizol (GIBCO/BRL), and cDNA was produced via reverse transcription. PCR was performed on cDNA by using primers specific for *KRIT1* (sense, 5′-TACATATGGGCTATAGTGCAC; antisense, 5′-TATCAGCTTAGCATCAGGAGCTG), yielding a 1,040-bp fragment. Primers for glyceraldehyde-3-phosphate dehydrogenase (GADPH) were used to control for RT-PCR efficiency and cDNA synthesis (sense, 5′-CCTCTGGAAAGCTGTGGCGT; antisense, 5′-TTGGAGGCCATGTAGGCCAT), yielding a 430-bp fragment.

KRIT1 Antibodies. Synthetic peptides corresponding to the following hydrophilic segments of KRIT1 were produced: peptide 1 (KRIT1 259–275), DYSKIQIPKQEKWQRS; peptide 2 (KRIT1 473–490), QLEPYHKPLQHVRDWPE; and peptide 3 (KRIT1 724–736, C terminus), *GGG*KLNGQLMATERNS. After conjugation to keyhole limpet hemocyanin (KLH), peptides were injected into rabbits and boosted twice; resulting antipeptide antibodies were affinity purified by using the immunizing peptide (Zymed). Antibody specificity was tested by Western blotting.

Western Blot. COS7 cells expressing His-tagged KRIT1 (expected size 62 kDa) from a pcDNA4/HisMax/Xpress plasmid (Invitrogen) were lysed and the products fractionated by SDS/PAGE. Antibodies were applied to resulting membranes and visualized by chemiluminescence (ref. 32; NEN).

For protein extraction from endothelial cells, cells were scraped directly into boiling sample buffer (100 mM Tris, pH 6.8/200 mM DTT/4% SDS/0.2% bromophenol blue/20% glyc-

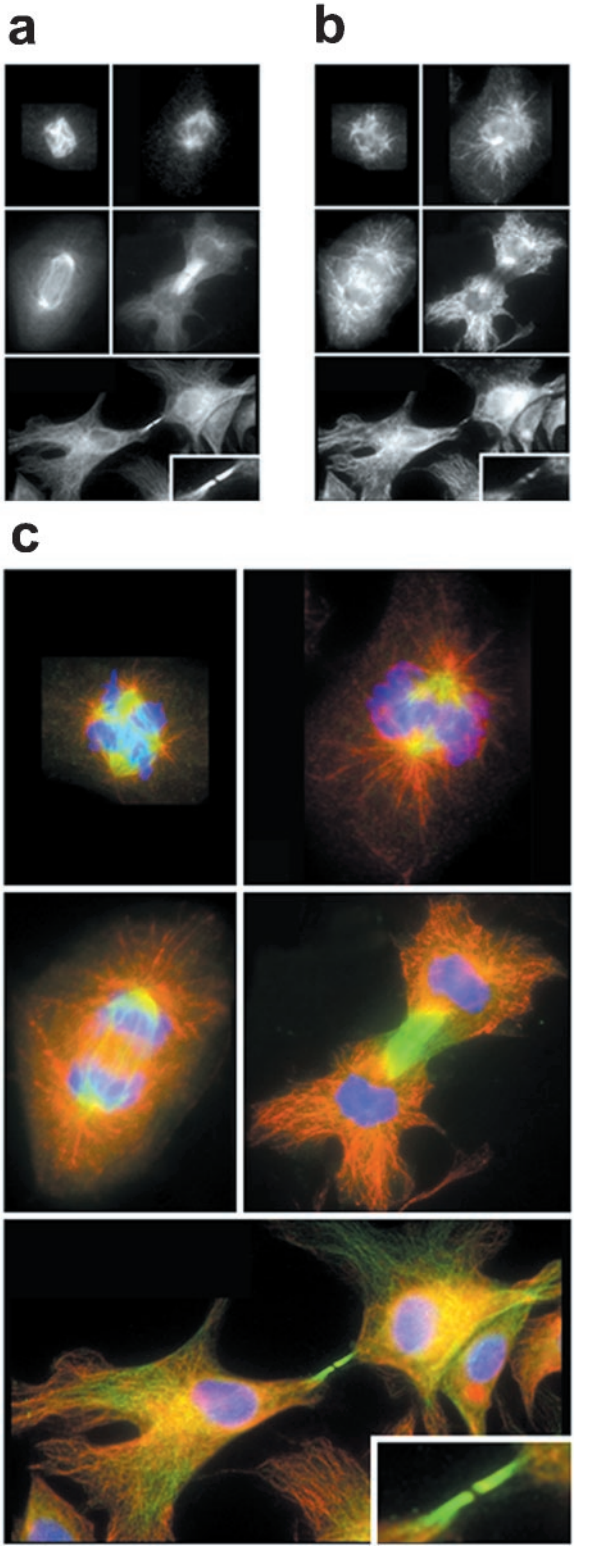

Fig. 5. KRIT1 and α-tubulin staining in mitosis. Cultured endothelial cells were stained with antibodies to KRIT1 (*a*) and antibodies to α-tubulin (*b*). In the composite image (*c*), KRIT1 staining is green and α-tubulin staining is red; yellow color indicates colocalization. During prometaphase and metaphase, antibodies to KRIT1 intensely stain the spindle pole bodies and the mitotic spindle. As cells progress through anaphase and into telophase, KRIT1 staining is most striking in the central portion of the midbody. In late telophase, KRIT1 localizes to the midbody remnant, consistent with the presence of KRIT1 at microtubule plus ends.

erol) before loading on gels. For SDS/PAGE, protein samples were fractionated by electrophoresis on a 10% acrylamide gel and transferred to membrane. Blots were blocked in 10% nonfat dried milk in PBS with 0.05% Tween 20. Blots were incubated with primary antibody, and staining was detected by incubation with horseradish peroxidase (HRP) donkey anti-rabbit antibody followed by chemiluminescence. For peptide competition assays, primary antibody was competed by a 4-fold molar excess of the immunizing peptide before incubation.

Immunoprecipitation. For immunoprecipitation, adherent BAECs were grown to confluency and lysed in ice-cold cytoskeletal lysis buffer (0.5% Nonidet P-40/10 mM Pipes, pH 6.8/50 mM NaCl/300 mM sucrose/3 mM $MgCl_2$) with protease inhibitors [4-(2-aminoethyl)benzenesulfonyl fluoride (AEBSF), pepstatinA, E-64, bestatin, leupeptin, and aprotinin; Sigma]. The lysate was precleared with Protein G Plus-Agarose (Oncogene, La Jolla, CA), after which β-tubulin antibody (developed by M. Klymkowsky, obtained from the Developmental Studies Hybridoma Bank developed under the auspices of the National Institute of Child Health and Human Development and maintained by the University of Iowa, Department of Biological Sciences, Iowa City) or KRIT1 antibody, separately coupled to Protein G Plus Agarose, was used for immunoprecipitation. After overnight incubation at 4°C, beads were collected by centrifugation, washed with lysis buffer, boiled and fractionated by SDS/PAGE, and analyzed by Western blotting as described above.

Immunocytochemistry. Cells were split onto microscope slides and grown for 24 h. The slides were washed with PBS, fixed with 3% paraformaldehyde, and permeabilized in 0.2% Triton X-100 in PBS. The sections were blocked with 10% normal donkey serum (NDS) and 1% BSA in PBS. They were incubated with primary followed by secondary antibody, stained with 4′,6-diamidino-2-phenylindole (DAPI) and mounted. β- and α-tubulin primary antibodies were purchased from Sigma. For actin staining, cells were incubated with 1 μM Phallodin (Sigma) conjugated to rhodamine. For cold-induced fracture of microtubules, BAECs were incubated in ice cold PBS for varying amounts of time and allowed to recover at 37°C, followed by immunocytochemistry.

Results

KRIT1 Is Expressed in Endothelial Cells. Antibodies to KRIT1 peptides were produced and affinity purified as described in *Methods*. Resulting antibodies were tested for specificity by Western blotting and immunohistochemistry. Antibodies directed against the 13-aa peptide at the C terminus of the protein specifically stained a peptide of the expected size in extracts of COS7 cells transfected with a His-tagged KRIT1 construct (Fig. 2*a*). This staining is competed with the immunizing peptide (Fig. 2*b*) demonstrating its specificity. This antibody also identified a product of the expected size for endogenous KRIT1 in untransfected BAECs (Fig. 2*c*). RT-PCR analysis confirmed the presence of *KRIT1* mRNA (Fig. 2*d*) in BAECs, and the sequence of this product identified it as the *KRIT1* ortholog (86% nucleotide and 85% amino acid sequence identity to human KRIT1).

KRIT1 Is Associated with Microtubules. We localized KRIT1 in BAECs by immunocytochemistry. During interphase, we observed that KRIT1 localized to the cytoplasm with a pattern suggesting association with a component of the cytoskeleton. To further characterize this pattern, we used double and triple staining with antibodies directed against KRIT1 and either actin or tubulin (Fig. 3*a*). KRIT1 showed colocalization with tubulin, but not with actin (Fig. 3*a*). Confocal microscopy confirmed the same pattern of colocalization with KRIT1, showing a granular staining pattern along the length of microtubules (Fig. 3*b*).

This association of KRIT1 with tubulin was further explored

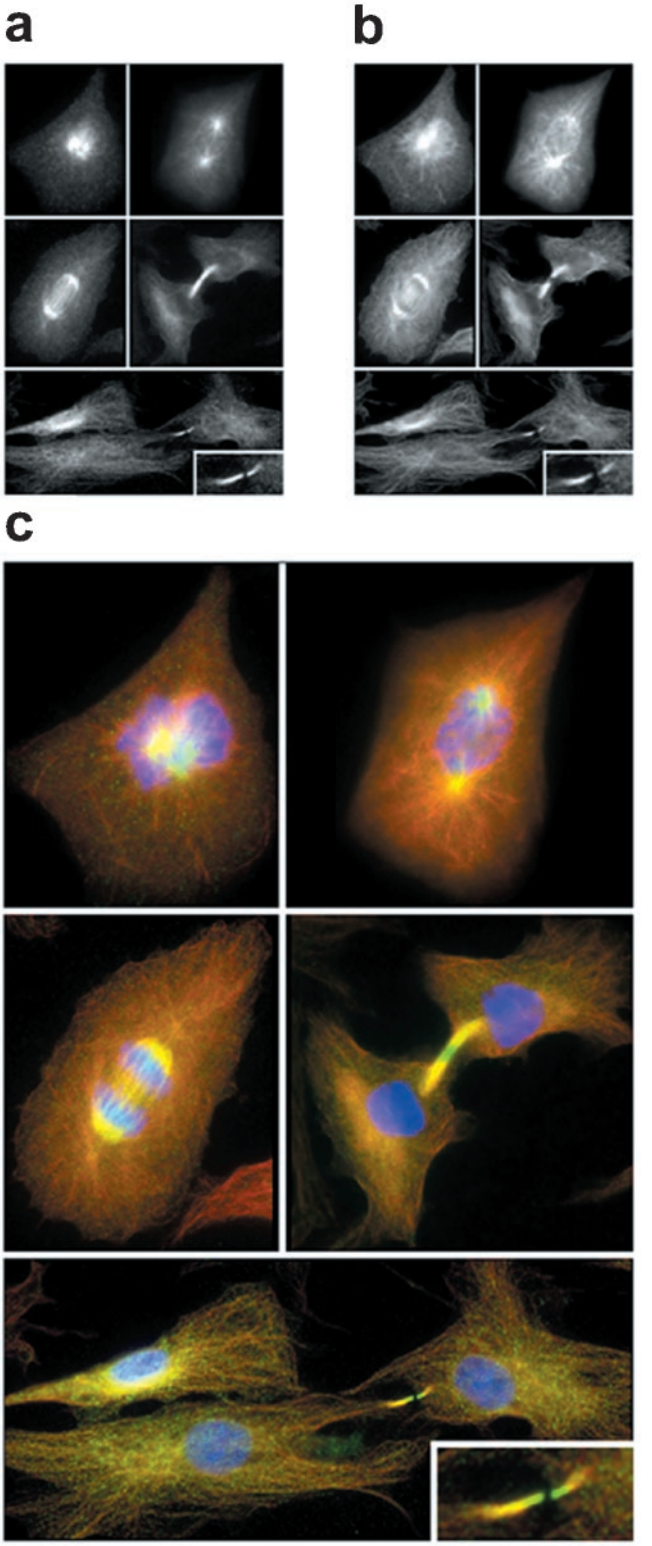

Fig. 6. KRIT1 and β-tubulin staining in mitosis. Cultured endothelial cells were stained with antibodies to KRIT1 (*a*) and antibodies to β-tubulin (*b*). In the composite image (*c*), KRIT1 staining is green and β-tubulin is red; yellow color indicates colocalization. During prometaphase and metaphase, antibodies to KRIT1 intensely stain the spindle pole bodies and the mitotic spindle. As cells progress through anaphase and into telophase, KRIT1 staining is most striking in the central portion of the midbody. In late telophase, KRIT1 localizes to the midbody remnant, extending beyond β-tubulin staining, consistent with the presence of KRIT1 at microtubule plus ends.

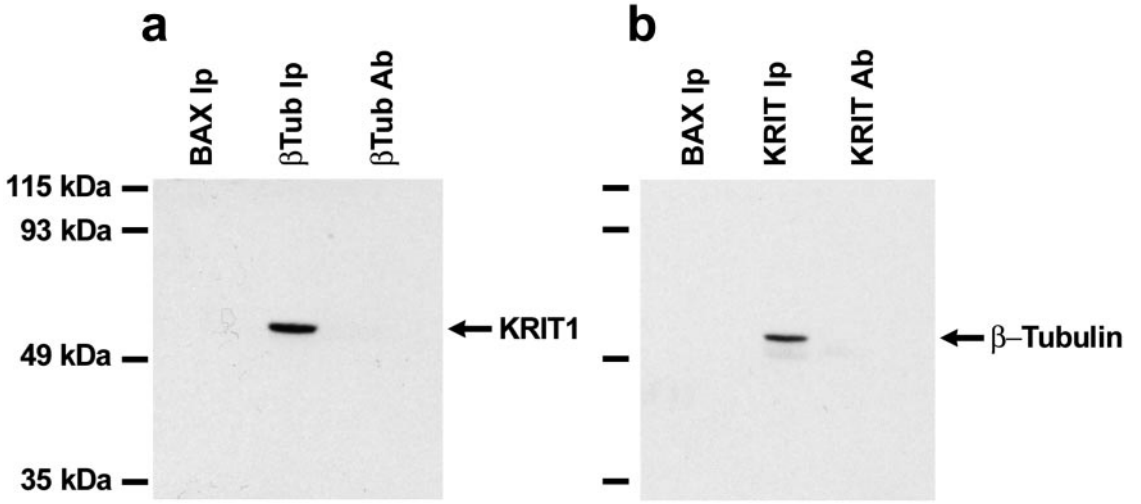

Fig. 7. KRIT1 and β-tubulin coimmunoprecipitate. (*a*) BAEC lysates were immunoprecipitated with mouse anti-Bax (lane 1), or mouse anti-β-tubulin (lane 2). Lane 3 has been loaded with an amount of β-tubulin antibody equal to that in lane 2 but no cell lysate. Western blots were prepared and probed with rabbit anti-KRIT1 antibody. The results demonstrate a band the size of KRIT1 only when lysate is precipitated with anti-β-tubulin. (*b*) BAEC lysates were immunoprecipitated with rabbit anti-Bax in lane 1 and rabbit anti-KRIT1 in lane 2. An equal amount of KRIT1 antibody has been loaded in lane 3. Western blots were prepared and probed with mouse antibody to β-tubulin. The results demonstrate a band the size of β-tubulin only when the lysate is precipitated with KRIT1.

by disruption of microtubules with cold (Fig. 4). The continued colocalization with tubulin demonstrates the association of KRIT1 and tubulin when polymerized (Figs. 3 and 4) and suggests that KRIT1 is a microtubule-associated protein.

Distribution of KRIT1 Protein in Mitotic Cells. To further explore the association of KRIT1 with microtubules, we investigated endothelial cells throughout mitosis. During metaphase, KRIT1 staining was most intense at the spindle pole bodies and the plus ends of the astral microtubules at the kinetochore of the mitotic spindle, paralleling the location of microtubule structures (Figs. 5 and 6). Similarly, during anaphase A, when chromosomes are separated by shrinking of kinetochore fibers, the region of the overlapping plus ends of the interpolar microtubules of the interzone showed strong KRIT1 staining (Figs. 5 and 6), here consistent with plus end association. Finally, the staining pattern was particularly striking in late telophase, during which KRIT1 localization is prominent at the midbody remnant, the site of cytokinesis where the extreme plus ends of microtubules of the two dividing cells overlap (Figs. 5 and 6). At these locations, KRIT1 staining can be seen to extend beyond the tip of tubulin expression (Fig. 6). This result is consistent with KRIT1's location at the extreme plus end of microtubules.

KRIT1 and β-Tubulin Coimmunoprecipitate. To determine whether KRIT1 and β-tubulin can be found together in a physical complex *in vivo*, coimmunoprecipitation experiments were performed. Either KRIT1 or β-tubulin antibody was used for immunoprecipitation from BAEC lysates; the precipitated protein was evaluated by Western blotting using these same antibodies. Complexes immunoprecipitated with β-tubulin antibodies contain KRIT1 (Fig. 7*a*). Conversely, complexes immunoprecipitated with antibodies to KRIT1 contain β-tubulin (Fig. 7*b*). In contrast, control antibodies directed against proteins not believed to form a complex with either KRIT1 or β-tubulin are not found in these complexes (Fig. 7).

Discussion

Microtubules are highly dynamic structures important in determining cellular morphology. The targeting and attachment of these polar structures appears to be directed by microtubule-associated proteins. Microtubules are nucleated at minus ends originating at the centrosome/microtubule-organizing center; these minus ends are enriched in α-tubulin. Growth and shrinkage occur at microtubule plus ends, which are enriched in β-tubulin; these plus ends explore the intracellular space and can be guided toward specialized membrane domains and chromosomes by specific plus-end-tracking proteins (33). We have shown that KRIT1 is a microtubule-associated protein that demonstrates increased localization to microtubule plus ends during mitosis. Immunoprecipitation experiments confirm that KRIT1 and β-tubulin are present within the same complexes, although they do not necessarily indicate a direct interaction.

The finding that KRIT1 can be located at microtubule plus ends suggests a potential role in targeting of microtubules, and the phenotype resulting from loss of KRIT1 function suggests a possible model for development of CCM lesions. One of the first stages of angiogenesis involves tube formation by endothelial cells; this tubulogenesis is triggered by interactions of endothelial cells with one another and with the extracellular matrix. Intercellular adhesion via PECAM1 (platelet endothelial cell adhesion molecule-1) provides signaling essential for endothelial tube formation (34, 35). It is intriguing that the GTPase activity of Krev1, an interacting partner of KRIT1 (28), is specifically activated by this interaction. This finding suggests a potential signaling pathway connecting cell–cell contact via PECAM1 to the microtubule cytoskeleton via Krev1 and KRIT1. Such a connection involving Krev1 and the cytoskeleton has been made in yeast, in which the sole homologue of Krev1 is *Bud1/RSR1*, which is required for normal selection of the budding site, a process that involves targeting of microtubules (36). Similarly, ICAP1 α, the other known KRIT1-interacting protein, is known to bind to the cytoplasmic C terminus of β1-integrin, thereby communicating information about cell–matrix interaction to the cell interior (30, 31). Consequently, the link between KRIT1 and microtubules on the one hand and KRIT1 with Krev1 and ICAP1 α on the other provides a potential pathway for signals from cell–cell contact and cell–matrix interaction, respectively, to influence cytoskeletal structure. The loss of this function could lead to the abnormal capillary development seen in patients with CCM because of impaired microtubule targeting, resulting in impaired tubulogenesis.

This proposed function of KRIT1 in targeting microtubules in response to external signals is reminiscent of that of EB1, another plus end microtubule-binding protein. EB1 binds to the tumor suppressor adenomatosis polyposis coli (APC), and it has been proposed that the activity of the Wnt signaling pathway is involved in the regulation of this interaction and the consequent targeting of microtubules (37).

These findings together provide localization of KRIT1 and also provide a framework for understanding the mechanism by which loss of KRIT1 causes human disease. Further work will be required to establish a role for KRIT1 in microtubule targeting and in determining the specific roles of other molecules involved in this pathway.

We thank Matthew State, Pietro de Camilli, Peter Takizawa, and Ketu Mishra-Gorur for helpful discussions. This work was supported by National Institutes of Health Grant R01-NS36194-05 (to R.P.L.).

1. Russell, D. S. & Rubenstein, L. J. (1989) *Pathology of Tumors of the Nervous System* (Williams & Wilkins, Baltimore), pp. 730–736.
2. Perl, J. & Ross, J. (1993) in *Cavernous Malformations*, eds. Awad, I. A. & Barrow, D. (Am. Assoc. Neurol. Surg., Rolling Meadows, IL), pp. 37–48.
3. Robinson, J. R., Awad, I. A. & Little, J. R. (1991) *J. Neurosurg.* **75,** 709–714.
4. Del Curling, O., Kelly, D. L., Elster, A. D. & Craven, T. E. (1991) *J. Neurosurg.* **75,** 702–708.
5. Sage, M. R., Brophy, B. P., Sweeney, C., Phipps, S., Perrerr, L. V., Sandhu, A. & Albertyn, L. E. (1993) *Australas. Radiol.* **37,** 147–155.
6. Otten, P., Pizzolato, G. P., Rilliet, B. & Berney, J. (1989) *Neurochirurgie* **35,** 82–83.
7. McCormick, W. F. & Boulter, T. R. (1966) *J. Neurosurg.* **25,** 309–311.
8. Zabramski, J. M., Wascher, T. M., Spetzler, R. F., Johnson, B., Golfinos, J., Drayer, B. P., Brown, B., Rigamonti, D. & Brown, G. (1994) *J. Neurosurg.* **80,** 422–432.
9. Robinson, J. R., Awad, I. A., Magdinec, M. & Paranandi, L. (1993) *Neurosurgery* **32,** 730–735; discussion 735–736.
10. Maraire, J. N. & Awad, I. A. (1995) *Neurosurgery* **37,** 591–605.
11. Barrow, D. & Awad, I. A. (1993) in *Cavernous Malformations*, eds. Awad, I. A. & Barrow, D. (Am. Assoc. Neurol. Surg., Rolling Meadows, IL), pp. 205–213.
12. Barrow, D. & Krisht, A. (1993) in *Cavernous Malformations*, eds. Awad, I. A. & Barrow, D. (Am. Assoc. Neurol. Surg., Rolling Meadows, IL), pp. 65–80.
13. Huhn, S., Rigamonti, D. & Hsu, F. (1993) in *Cavernous Malformations*, eds. Awad, I. A. & Barrow, D. (Am. Assoc. Neurol. Surg., Rolling Meadows, IL), pp. 87–99.
14. Michael, J. C. & Levin, P. M. (1936) *Arch. Neurol. Psychiatry* **36,** 514–536.
15. Kidd, H. A. & Cumings, J. N. (1947) *Lancet* **I,** 747–748.
16. Hayman, L. A., Evans, R. A., Ferrell, R. E., Fahr, L. M., Ostrow, P. & Riccardi, V. M. (1982) *Am. J. Med. Genet.* **11,** 147–160.
17. Gunel, M., Awad, I. A., Finberg, K., Steinberg, G. K., Craig, H. D., Cepeda, O., Nelson-Williams, C. & Lifton, R. P. (1996) *Neurosurgery* **38,** 1265–1271.
18. Craig, H. D., Gunel, M., Cepeda, O., Johnson, E. W., Ptacek, L., Steinberg, G. K., Ogilvy, C. S., Berg, M. J., Crawford, S. C., Scott, R. M., *et al*. (1998) *Hum. Mol. Genet.* **7,** 1851–1858.
19. Marchuk, D. A., Gallione, C. J., Morrison, L. A., Clericuzio, C. L., Hart, B. L., Kosofsky, B. E., Louis, D. N., Gusella, J. F., Davis, L. E. & Prenger, V. L. (1995) *Genomics* **28,** 311–314.
20. Johnson, E. W., Iyer, L. M., Rich, S. S., Orr, H. T., Gil-Nagel, A., Kurth, J. H., Zabramski, J. M., Marchuk, D. A., Weissenbach, J., Clericuzio, C. L., *et al*. (1995) *Genome Res.* **5,** 368–380.
21. Dubovsky, J., Zabramski, J. M., Kurth, J., Spetzler, R. F., Rich, S. S., Orr, H. T. & Weber, J. L. (1995) *Hum. Mol. Genet.* **4,** 453–458.
22. Laberge-le Couteulx, S., Jung, H. H., Labauge, P., Houtteville, J. P., Lescoat, C., Cecillon, M., Marechal, E., Joutel, A., Bach, J. F. & Tournier-Lasserve, E. (1999) *Nat. Genet.* **23,** 189–193.
23. Sahoo, T., Johnson, E. W., Thomas, J. W., Kuehl, P. M., Jones, T. L., Dokken, C. G., Touchman, J. W., Gallione, C. J., Lee-Lin, S. Q., Kosofsky, B., *et al*. (1999) *Hum. Mol. Genet.* **8,** 2325–2333.
24. Eerola, I., Plate, K. H., Spiegel, R., Boon, L. M., Mulliken, J. B. & Vikkula, M. (2000) *Hum. Mol. Genet.* **9,** 1351–1355.
25. Lucas, M., Solano, F., Zayas, M. D., Garcia-Moreno, J. M., Gamero, M. A., Costa, A. F. & Izquierdo, G. (2000) *Ann. Neurol.* **47,** 836.
26. Zhang, J., Clatterbuck, R. E., Rigamonti, D. & Dietz, H. C. (2000) *Neurosurgery* **46,** 1272–1277; discussion 1277–1279.
27. Davenport, W. J., Siegel, A. M., Dichgans, J., Drigo, P., Mammi, I., Pereda, P., Wood, N. W. & Rouleau, G. A. (2001) *Neurology* **56,** 540–543.
28. Serebriiskii, I., Estojak, J., Sonoda, G., Testa, J. R. & Golemis, E. A. (1997) *Oncogene* **15,** 1043–1049.
29. Rak, J., Mitsuhashi, Y., Bayko, L., Filmus, J., Shirasawa, S., Sasazuki, T. & Kerbel, R. S. (1995) *Cancer Res.* **55,** 4575–4580.
30. Zhang, J., Clatterbuck, R. E., Rigamonti, D., Chang, D. D. & Dietz, H. C. (2001) *Hum. Mol. Genet.* **10,** 2953–2960.
31. Zawistowski, J. S., Serebriiskii, I. G., Lee, M. F., Golemis, E. A. & Marchuk, D. A. (2002) *Hum. Mol. Genet.* **11,** 389–396.
32. Roda, A., Pasini, P., Guardigli, M., Baraldini, M., Musiani, M. & Mirasoli, M. (2000) *Fresenius J. Anal. Chem.* **366,** 752–759.
33. Schuyler, S. C. & Pellman, D. (2001) *Cell* **105,** 421–424.
34. Albelda, S. M., Muller, W. A., Buck, C. A. & Newman, P. J. (1991) *J. Cell Biol.* **114,** 1059–1068.
35. Reedquist, K. A., Ross, E., Koop, E. A., Wolthuis, R. M., Zwartkruis, F. J., van Kooyk, Y., Salmon, M., Buckley, C. D. & Bos, J. L. (2000) *J. Cell Biol.* **148,** 1151–1158.
36. Ruggieri, R., Bender, A., Matsui, Y., Powers, S., Takai, Y., Pringle, J. R. & Matsumoto, K. (1992) *Mol. Cell. Biol.* **12,** 758–766.
37. Juwana, J. P., Henderikx, P., Mischo, A., Wadle, A., Fadle, N., Gerlach, K., Arends, J. W., Hoogenboom, H., Pfreundschuh, M. & Renner, C. (1999) *Int. J. Cancer* **81,** 275–284.